Inorganica Chimica Acta 514 (2021) 120021

Contents lists available at ScienceDirect

Inorganica Chimica Acta

journal homepage: www.elsevier.com/locate/ica

Research paper

Salicylimine-based fluorescent chemosensor for magnesium ions in aqueous solution

Reza Azadbakht[a,*], Mostafa Koolivand[b], Saeid Menati[c]

[a] Faculty of Chemistry, Bu-Ali Sina University, Hamedan 65174, Iran
[b] Department of Chemistry, Payame Noor University, Tehran, Iran
[c] Department of Chemistry, Khorramabad Branch, Islamic Azad University, Khorramabad, Iran

ARTICLE INFO

Keywords:
Magnesium
Salicylimine-based receptor
C=N isomerization
Chemosensor

ABSTRACT

A new fluorescent schiff base chemosensor (H_2L) was prepared for the sensitive and selective sensing of Mg^{2+} ions based on multiple mechanisms. H_2L is a weak fluorescent (f = 0.031) due to PET process and C=N isomerization. Upon addition of Mg^{2+}, the complex [MgL] was formed and a remarkable fluorescence enhancement (f = 0.182) was produced. H_2L had no such significant effect on the fluorescence in the presence of metal ions, such as Na^+, Ag^+, K^+, Ca^{2+}, Mg^{2+}, Hg^{2+}, Mn^{2+}, Co^{2+}, Ni^{2+}, Cu^{2+}, Zn^{2+}, Cd^{2+}, Pb^{2+}, Cr^{3+}, Fe^{3+}, and In^{3+}. The satisfactory linear relationship was observed between the added concentrations of Mg^{2+} and the fluorescence intensity of H_2L. The detection limit was 3.04×10^{-9} M with a rapid response time. Chemical inputs of Mg^{2+} and Fe^{3+} ions satisfy the conditions of INHIBIT molecular logic gate.

1. Introduction

Magnesium is one of the vital cofactors that participates in a lot of biochemical reactions including protein synthesis, muscle and nerve function, blood glucose control and blood pressure regulation [1]. Magnesium is also necessary for the synthesis of DNA and RNA, the antioxidant glutathione, oxidative phosphorylation, normal heart rhythm, muscle contraction, the structural development of bone, glycolysis and energy production [2]. Diseases such as Alzheimer, diabetes, hypertension, and epilepsy have relation with abnormal concentrations of magnesium in the cytosol and subcellular regions [3–6]. Therefore, finding an efficient analytical and simple technique for imaging and detection of magnesium is of great interest [7]. Fluorescence chemosensors offer a number of outstanding characteristics such as real-time response and simple handling allowing dynamic measurements. In recent years, considerable efforts have been spent on developing of new suitable fluorescent probes matching all desired properties such as easy preparation, selectivity, high sensitivity, low-cost synthesis and aqueous solubility [8–17]. Designing of chemosensors for Mg^{2+} have been attracting increasing interest based on the fluorescence signaling mechanisms such as intramolecular charge transfer (ICT) [18], C=N isomerization [19], photoinduced electron transfer (PET) [20], appropriate cavities [21], excited-state intra-/intermolecular proton transfer (ESIPT) [22]. The photoinduced electron transfer (PET) mechanism is the process by which an electron falls from an excited site to a site with lower energy. The matching of their oxidation–reduction potentials of the two sites and the closeness in space are necessary requirements for this transport. The mechanism of isomerization related to molecules which are easily isomerize in the excited state but highly stable in the ground state. The isomerization mechanism has been observed for several classes of molecules. Schiff base compounds are one of the classical examples for isomerization mechanism. Furthermore, because of the strong binding abilities to various metal ions and the individual photophysical properties, Schiff base derivatives have been extensively explored in the field of the field of chemosensors for detection of metal ions [23–27]. In this work, a π-conjugated Schiff base receptor (H_2L) was designed and synthesized. The photophysical studies showed that H_2L can be used as a selective and sensitive chemosensor for Mg^{2+} ions by enhancement of fluorescence emission intensity in EtOH/H_2O (9:1, v/v, pH = 7.40). H_2L exhibits rapid response, low detection limit (3.04×10^{-9} M), excellent selectivity and sensitivity to Mg^{2+}.

2. Experimental

2.1. Materials and instruments

All solvents commercially purchased and were of reagent grade quality. 1,2-diamino ethane, 1-chloro-2-nitrobenzene and 2-hydroxybenzaldehyde were obtained from Merck and was used without any

* Corresponding author.
E-mail address: r_azadbakht@yahoo.com (R. Azadbakht).

https://doi.org/10.1016/j.ica.2020.120021
Received 23 June 2020; Received in revised form 13 September 2020; Accepted 13 September 2020
Available online 18 September 2020

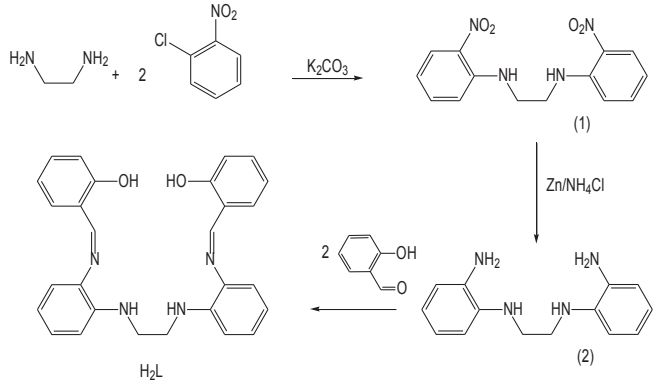

Scheme 1. The synthetic route of H_2L.

further purification. A Bruker A V300 MHz spectrometer was used to obtain NMR spectra. A BIO-RAD FTS-40A spectrophotometer was used to record infrared spectra in KBr pellets (4000–400 cm^{-1}). A Kratos-MS-50 spectrometer was used to record positive ion FAB mass spectra with 3-nitrobenzyl alcohol as the matrix solvent. A Varian Cary Eclipse 300 spectrophotometer was used to obtain UV–Vis absorption spectra. The fluorescence spectra were recorded on a Varian spectrofluorometer. Both emission and excitation bands were set at 5 nm.

2.2. N,N'-bis(2-nitrophenyl)-1,2-ethanediamine (1)

Potassium carbonate (2.76, 20 mmol), 1-chloro-2-nitrobenzene (3.14 g, 20 mmol) and 1,2-diaminoethane (0.64 g, 10 mmol) were completely mixed in a round-bottomed flask. The reaction was heated at 175 °C in an oil bath for 3 h. After cooling, the yellow solid was collected and washed by 3:1 H_2O/EtOH (×3). Yield (82%), Scheme 1. Anal. Calc. for $C_{14}H_{14}N_4O_4$: C, 55.63; H, 4.67; N, 18.53. Found: C, 55.82; H, 4.70; N, 18.49%. IR (KBr, cm^{-1}) 1350, 1570 m (NO_2), 3360(NH); ^{1}HNMR δ_H ($CDCl_3$, ppm) 3.40 (t, 4H, CH_2–CH_2), 6.70 (m, 4H, Ar), 7.35(t, 2H, Ar), 7.90 (d, 2H, Ar), 7.35 (t, 2H, NH).

2.3. N,N'-bis(2-aminophenyl)-1,2-ethanediamine (2)

A mixture of ammonium chloride (4 g), 2-nitro-N-(2-(2-nitrophenylamino)propyl)benzenamine (3.16 g, 10 mmol), and H_2O (2 ml) in 100 ml of ethanol was heated to boiling and then 3 g of zinc dust were gradually added over a period of 0.5 h. When the color of the solution changed from brown to pale yellow, it was filtered and washed. Distilled water (1000 ml) was added to the filtrated solution and the pH was adjusted to 12 with potassium hydroxide. The product as brown powder participates were appeared in the solution. Yield (1.3 g, 62%). Anal. Calc. for $C_{14}H_{18}N_4$: C, 69.39; H, 7.46; N, 23.12. Found: C, 69.20; H, 7.34; N, 23.32%. IR (KBr, cm^{-1}) 3452 and 3464 m (NH_2); 3344 m (NH); ^{1}H NMR δ_H ($CDCl_3$, ppm) 3.33 (br, 10*H*, CH_2–CH_2 and NH), 6.64 (m, 8H, Ar); ^{13}C NMR δC ($CDCl_3$, ppm) 40.0, 135.9, 134.7, 120.1, 118.0, 113.4, 109.1

2.4. Synthesis of H_2L

To a solution of 2-hydroxybenzaldehyde (0.24 g, 2 mmol) in absolute ethanol, N,N'-bis(2-aminophenyl)-1,2-ethanediamine (0.23 g, 1 mmol) was added and the reaction was gently refluxed approximately for 3 h. The product precipitating was filtered off and washed with ethanol, and dried in air at room temperature. Yield (70%). Anal. Calc. for $C_{36}H_{30}N_4O_2$: C, 74.65; H, 5.82; N, 12.44. Found: C, 74.88; H, 5.70; N, 12.61%. IR (KBr, cm^{-1}) 3412 (OH), 1621 (C═N);^{1}H NMR δ_H (DMSO-d_6, ppm) 3.52 (s, 4H, CH_2), 4.59 (s, 2H, NH) 6.74–7.37 (4 signals, 16H, Ar), 8.51 (s, CH = N, 2H), 12.82 (s, OH, 2H); ^{13}C NMR δC (DMSO-d_6, ppm) 43.08, 110.79, 117.10, 117.36, 118.31, 119.18, 128.32, 132.30, 132.99, 135.66, 141.83, 160.69 and162.51. The mass spectrum shows peak at m/z = 450.2 corresponding to the H_2L (Figs. S1–S4).

3. Results and discussion

3.1. Synthesis

H_2L was readily synthesized in 74% yield by condensation of N,N'-bis(2-aminophenyl)-1,2-ethanediamine and salicylaldehyde in ethanol (scheme 1). Its structure was investigated by mass, ^{1}HNMR, ^{13}C NMR spectra (see Figs. S1–S4, in the supporting information).

The main band appearing in the FTIR spectrum was related to stretching vibration of C═N bands and no bands attributable to C═O were observed. The stretch vibration of secondary amines (N—H) appear at *ca* 3396 cm^{-1}. In ^{1}H NMR spectrum, a singlet signal at 3.52 ppm and a broad signal at 4.59 ppm were appeared related to methylen protons and amine protons, respectively. A single ^{1}H imine resonance at 8.51 ppm was appeared demonstrating the equivalence of the two imine environments. The signal at 12.82 ppm can be attributed to the hydroxyl protons (the protons related to the intramolecular hydrogen bonds were appeared in very low-field proton resonance). Four signals have been observed in the aromatic region (6.74–7.37 ppm). In ^{13}C NMR spectrum, one signal at 43.08 ppm was observed attributed to methylene carbons. There is one type for the imine carbon atoms (162.51 ppm) demonstrating the equivalence of the two imine environments. Eleven peaks have been observed in the aromatic region (110.79–160.69 ppm).

From reaction if H_2L with $MgCl_2$, the complex of [MgL] was synthesized. The IR spectra of H_2L and [MgL] were prepared and compared. As can be seen from Fig. S3, two differences have been observed: (i) The absorption band at 3397 cm^{-1} corresponding to the N—H stretching vibration shifted to 3381 cm^{-1} (ii) the stretch vibration of imine group (C═N) at 1609 cm^{-1} shifted to 1624 cm^{-1}. These observations suggest that the imine groups and the amine groups may participate in the coordination interaction to Mg^{2+} ions.

3.2. Spectral properties of fluorescent H_2L

H_2L (10 μM) exhibits a weak fluorescence intensity around 490 nm when excited at 423 nm. The fluorescence emission measurements of H_2L were made at room temperature in different solvents: water, ethanol, methanol, chloroform, acetonitrile and dimethylformamide (DMF). Investigation of the solvent-dependent fluorescence emission - displayed that the fluorescence is strongly quenched in protic solvents. The magnitude of the quenching depends on the H bond- donating ability of the solvent (Fig. 1).

The salicylimine- derivatives are known to be good ligands for fluorescence studies and used to develop chemosensors. The excitation and emission wavelengths of the H_2L were found at higher wavelength, in compared to naphthalene groups. This red-shift is related to the delocalization the imine π-electrons on the aromatic amines results in a red-shift of the excitation and emission wavelengths of the related aromatic rings. The emission spectra of H_2L on excitation at 423 nm shows a broad band at 490 nm. The selective binding behavior of H_2L towards different metal nitrates (Na^+, K^+, Cs^+, Mg^{2+}, Ba^{2+}, Ca^{2+} Al^{3+}, Pb^{2+}, Mn^{2+}, Fe^{2+}, Fe^{3+}, Co^{2+}, Ni^{2+}, Cu^{2+}, Zn^{2+}, Cd^{2+}, Hg^{2+} and Ag^+) was studied by fluorescence spectroscopies. All of the titration experiments were carried out in EtOH/H_2O (9/1, v/v) upon adding the respective metal ions. Fig. 2 exhibits the changes in the fluorescence spectra of H_2L by addition of the various tested metal ions.

The complexation reaction occurs with formation of neutral complex [MgL] coupling with release of H^+ ions:

$$H_2L + Mg^{2+} \rightarrow [MgL] + 2H^+$$

It should be noted that H_2L molecules are functioning as charged

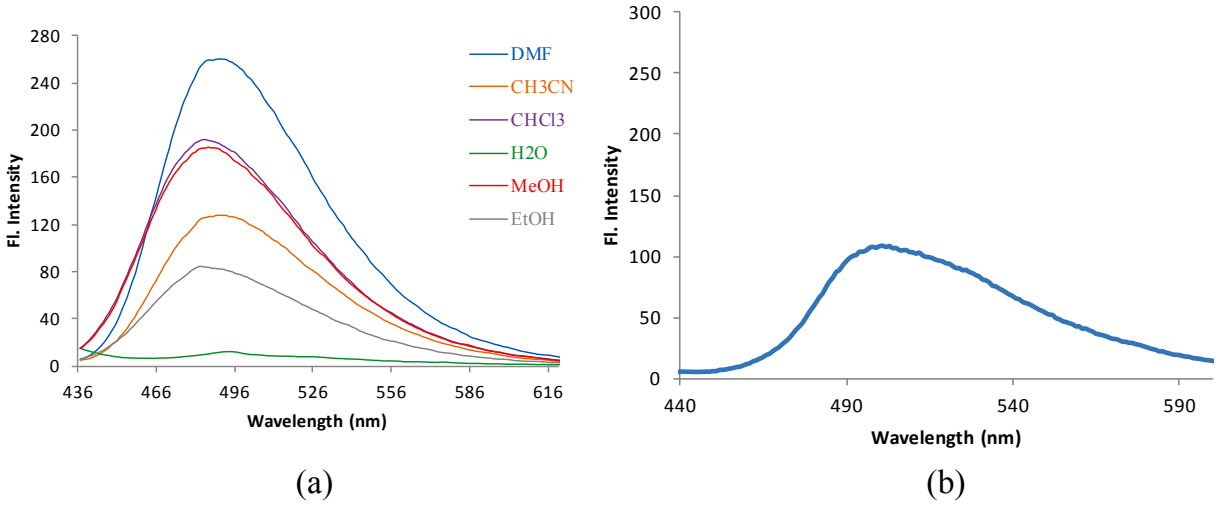

Fig. 1. (a) Changes of fluorescence spectrum of H_2L in different solvents, (b) solid-state fluorescence of H_2L. Excitation wavelength was 423 nm.

ionophore, thus taking into account stability constant of the complex the stability constant of [MgL] is pH dependent. Therefore, a few drops of triethylamine were added to the solution and then the selective binding behavior of H_2L towards different cations was studied (Fig. 3).

Among the tested metal ions (5.0 equiv), no significant spectral changes were observed in the presence of Na^+, K^+, Cs^+, Ba^{2+}, Ca^{2+} and Zn^{2+}, while a fluorescence quenching was seen upon the addition of Al^{3+}, Pb^{2+}, Mn^{2+}, Fe^{2+}, Fe^{3+}, Co^{2+}, Ni^{2+}, Cu^{2+}, Cd^{2+}, Hg^{2+} and Ag^+. However, a large enhancement in fluorescence intensity was only observed in the presence of Mg^{2+} ions.

The FEF (fluorescence enhancement factor) values of (H_2L + triethylamine) corresponding to different metal ions are shown in Fig. 4. The FEF (Ix- I_{H2L}/I_{H2L}) was calculated using minimal (I_{H2L}) and maximal (Ix) fluorescence intensities recorded before and after addition of metal ions at 490 nm, respectively. The highest fluorescence enhancement for (H_2L) has been observed in the presence of Mg^{2+} ions (Fig. 4).

To test practical applicability of H_2L as a fluorescence chemosensor for Mg^{2+}, competition experiments were carried out in the presence of other metal cations (Fig. 5). The results show that the fluorescence of H_2L upon complexation to Mg^{2+} did not significantly change in the presence of Na^+, K^+, Mg^{2+}, Ca^{2+}, Ba^{2+}, Al^{3+}, Co^{2+}, Ni^{2+}, Zn^{2+}, Cd^{2+}, Pb^{2+}, Cd^{2+}, and Hg^{2+} with a concentration up to 100 mM. In the presence of Mn^{2+}, Fe^{2+}, Cu^{2+}, Fe^{3+} and Ag^+ ions had a disturbance under their much excess.

The coordination mode of H_2L to Mg^{2+} was investigated by mixing various amounts of Mg^{2+} with a constant concentration of H_2L (Fig. 6). In the fluorescence titration experiments, the fluorescence emission intensity was gradually increased when 1 equivalent of Mg^{2+} was added, it no longer changed when the concentration of Mg^{2+} increased (Fig. 6, inset), indicating the 1:1 binding of H_2L to Mg^{2+} (Fig. 6).

To determine the binding stoichiometry of H_2L and Mg^{2+} ion, the job plot method was also used. The molar ratio was given by $[Mg^{2+}]/([Mg^{2+}] + [H_2L])$ and measured from 0 to 1. The total concentrations were kept at 10 μM. As seen in Fig. 7, the maximum value of the molar ratio was 0.5. This means that the molar ratio of the H_2L–Mg^{2+} complex was 1:1 in the binding stoichiometry.

Free H_2L shows a weak fluorescence emission because of existence the photo-induced electron transfer (PET) of the lone pair electrons from imine to the fluorophore in the excited state and the C=N isomerization. When Mg^{2+} was added a stable chelation of Mg^{2+} to H_2L inhibited PET process and C=N isomerization, resulting in a significant fluorescence emission.

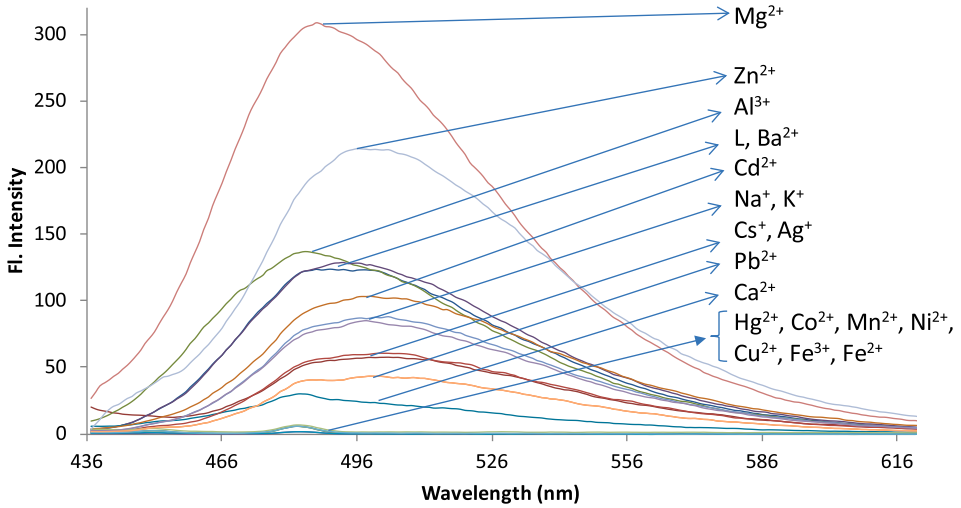

Fig. 2. Changes of fluorescence emission intensity of H_2L (10 μ M) upon addition of various metal ions (10 equiv) in EtOH/H_2O (9:1, v/v) containing HEPES buffer (10 mM, pH 7.4).

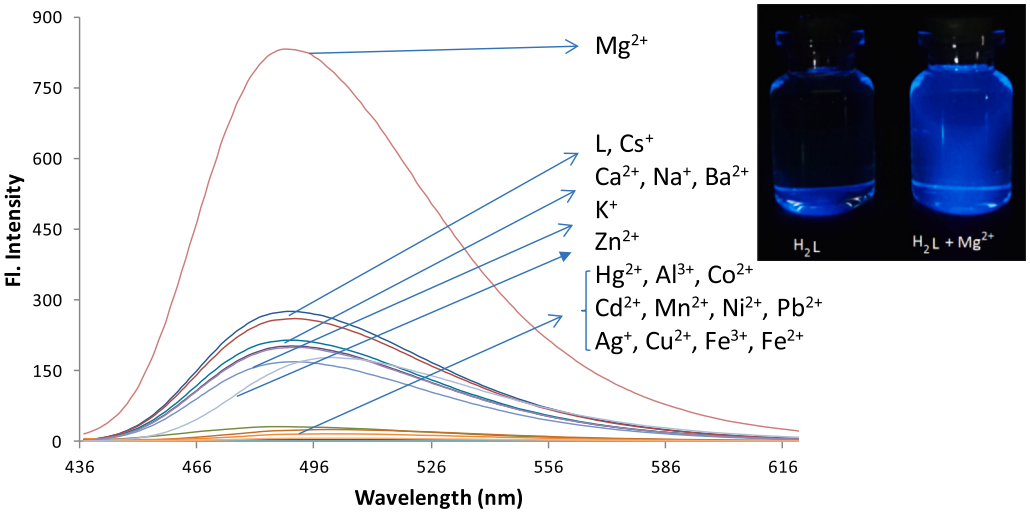

Fig. 3. Changes of fluorescence emission intensity of H_2L + trimethylamine in EtOH/H_2O (9:1, v/v; HEPES, pH 7.4) upon addition of various metal ions (10 equiv) with an excitation wavelength of 423 nm.

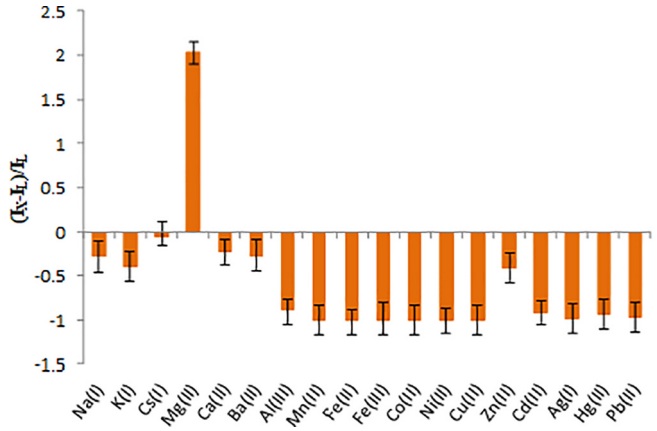

Fig. 4. The fluorescence enhancement factor (FEF) of (H_2L + triethylamine) upon addition of various metal ions in EtOH/H_2O (9:1, v/v; HEPES, pH 7.4) at 25 °C. Both the excitation and emission slit widths were 5.0 nm.

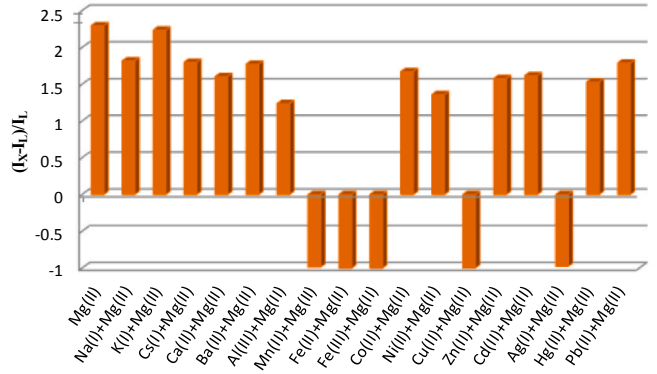

Fig. 5. The fluorescence enhancement factor (FEF) of (H_2L + triethylamine) upon addition of Mg^{2+} ions in the presence of various metal ions in EtOH/H_2O (9:1, v/v; HEPES, pH 7.4) at 25 °C. Both the excitation and emission slit widths were 5.0 nm.

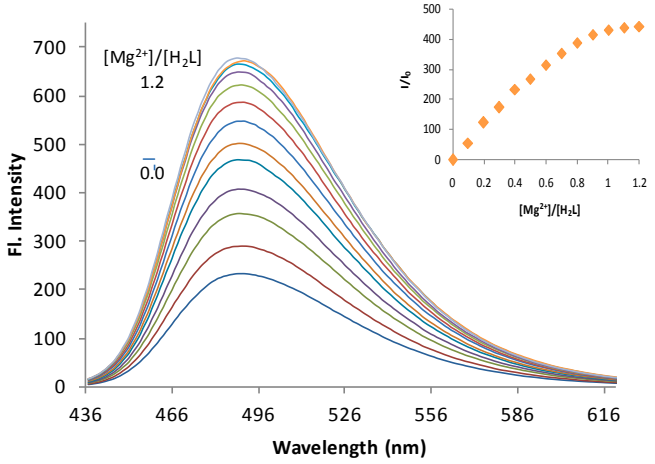

Fig. 6. The titration of (H_2L) (10 μM) as a function of added Mg^{2+} concentration in EtOH/H_2O (9:1, v/v). Excitation wavelength was 423 nm. Both the emission and excitation slit widths were 5.0 nm.

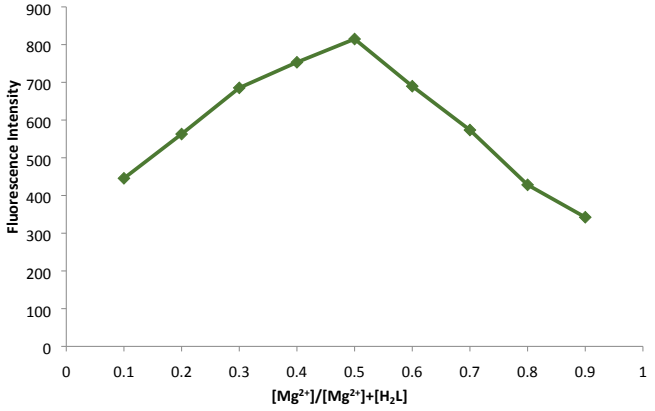

Fig. 7. Job's plot analysis of H_2L and Mg^{2+}.

3.3. NMR studies

The ^1H NMR spectra of H_2L were recorded in the absence and presence of and Mg^{2+} ions (Fig. 8) As shown in Fig. 8, upon the addition of Mg^{2+}, the resonance signals corresponding to imine protons shift downfield from 8.51 to 10.31 ppm, and the resonance signals corresponding to methylene protons shift downfield from 3.52 to 4.39 ppm. When Mg^{2+} was added, the signals corresponding to hydroxyl protons (–OH) were disappeared duo to deprotonation of the hydroxyl groups to strongly coordinate to Mg^{2+}. The proton signals of

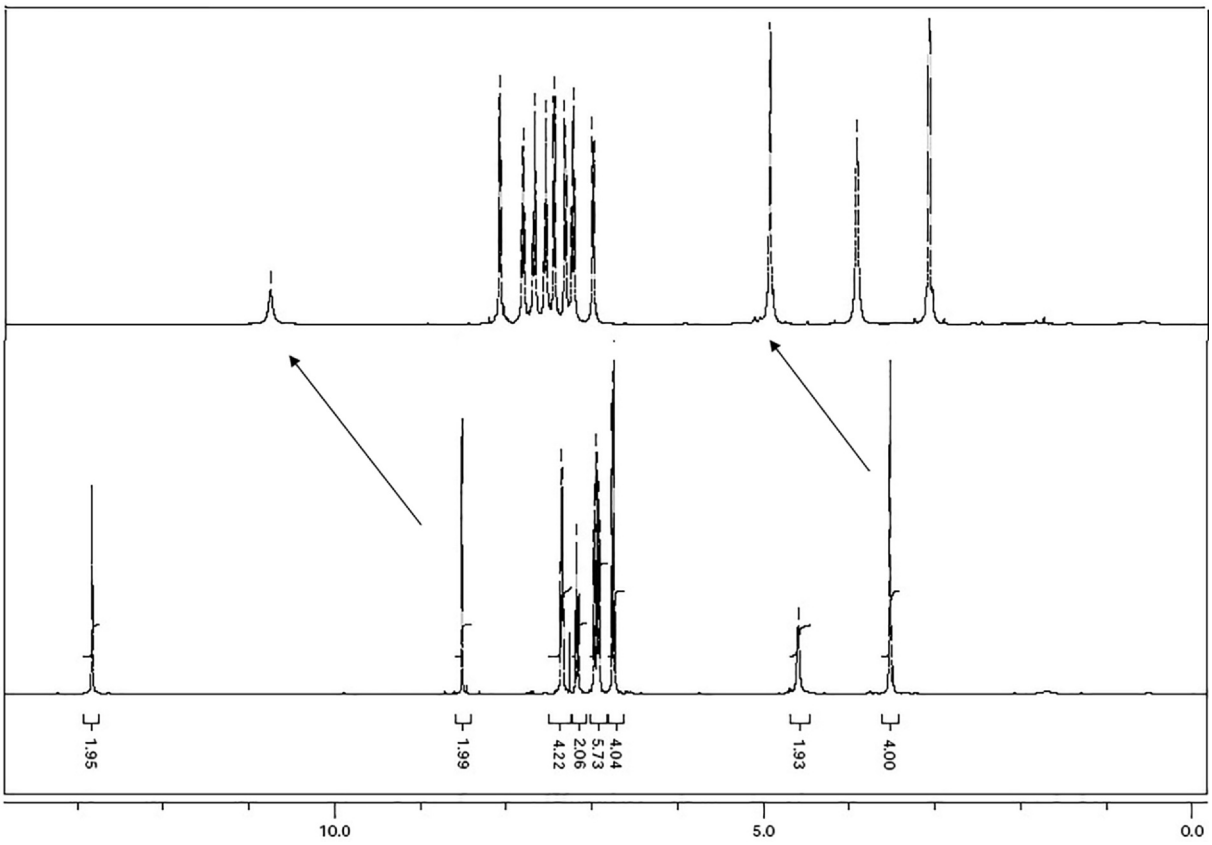

Fig. 8. ^{1}H NMR spectra of compound H_2L and its complex with Mg^{2+} ([MgL]) at room temperature.

NH (4.59 ppm) are exchanged with deuterium atoms of DMSO-d_6. This result indicats that a more efficient coordination of Mg^{2+} ion occurs with the imine nitrogen (C═N), the nitrogen (–NH) of ethylene diamine moiety and hydroxyl groups. When Mg^{2+} ion is coordinated to H_2L, the charge transfer was arrested due to the strong complexation of Mg^{2+} with H_2L. In addition, Mg^{2+} ion as a soft acid, preferentially interacts with the hydroxyl group and nitrogen atoms according to Pearson's HSAB theory.

3.4. Infrared studies

The IR spectrum of H_2L shows the bands at 1620 and 3381 cm^{-1} related to stretching vibrations of υ(C═N) and υ(N−H), respectively (Fig. 9). The band related to azomethine has been shifted to lower frequency 1609 cm^{-1} in the spectrum of the complex. This shift can be attributed to the coordination of nitrogen atoms of the azomethine group to the metal atom. This can be explained by the donation of electrons from bonding orbital C═N to the empty d-orbitals of the metal ion. The band related to secondry amine has been shifted to higher frequency 3391 cm^{-1} in the spectrum of the complex. The IR spectra of L also exhibited a band at 3263 cm^{-1}, which was attributed to the stretching vibration of υ (OH). In the spectrum of the complex, this absorption was disappeared, that expressed deprotonation and participation of the enol oxygen in coordination (Fig. 9). These evidences indicate that the nitrogen of azomethine and secondary groups and the oxygen of ligand are involved in chelation with metal ion.

3.5. Limit of detection and response time

The fluorescence titration was used to determine of the limit of detection. For this means, the equation of 3σ/s was applied where s is the slope of the calibration curve and σ is the standard deviation of the blank solution. As shown in Fig. 10, H_2L has a detection limit of 3.04×10^{-9} M for Mg^{2+}. The affinity and sensitivity of the probe towards Mg^{2+} in the presence of Ca^{2+} ions is a challenge for in vivo and in vitro monitoring of Mg^{2+} under intracellular conditions.

The concentration of Mg^{2+} in intracellular conditions is of the order 0.1–6 mmol L^{-1} whereas the intracellular concentration of Ca^{2+} may vary from 0.1 μmol L^{-1} to 1 mmol L^{-1}. This study shows that H_2L is a highly selective and sensitive fluorescent chemosensor to recognize of Mg^{2+} without the interference of other metal ions, especially Ca^{2+}. The response time is a necessary and important factor for fluorescence chemosensors. The response time of the chemosensor was studied by the kinetics of fluorescence enhancement at 358 nm. The response time to Mg^{2+} is less than 5 s. Fast changes in the fluorescence intensity of the chemosensor were appeared and remained quite stable when H_2L was titrated with magnesium ions.

3.6. Binding constants measurements

The association constant (K_a) of H_2L with Mg^{2+} was calculated from the Benesi–Hildebrand plot. The fluorescent titration spectra of H_2L (10 μM) in the presence of various concentrations of Mg^{2+} (0–1.2 μM) were conducted. When Mg^{2+} ions were increased, the fluorescence intensity emission of the solution was increased (Fig. 11). It should be noted that at more than 10 μM of Mg^{2+}, the fluorescence intensity reached to the constant value.

$$\frac{1}{I - I_0} = \frac{1}{K_a (I_{max} - I_0)[Mg^{2+}]} - \frac{1}{I_{max} - I_0}$$

where I and I_0 represent the emission intensity of H_2L in the presence and absence of Mg^{2+}, respectively, I_{max} is the saturated emission of H_2L in the presence of excess amount of Mg^{2+}; $[Mg^{2+}]$ is the concentration of Mg^{2+} ion added. The measured emission intensity $[1/(I - I_0)]$ varied as a function of $1/[Mg^{2+}]$ in a linear relationship ($R^2 = 0.99$),

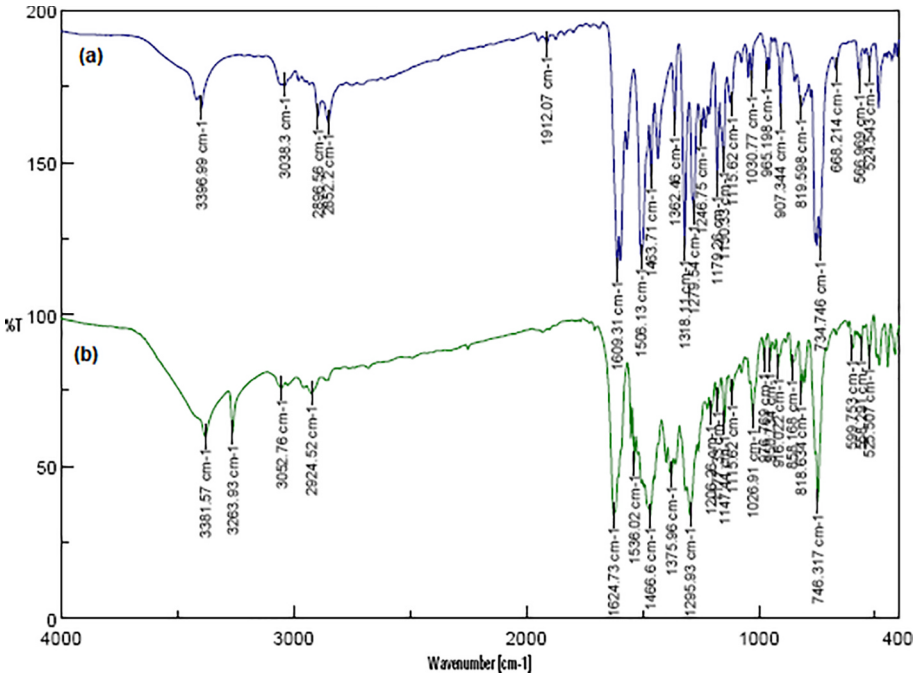

Fig. 9. The comparison between the IR spectra of (a) [MgL], (b) H_2L.

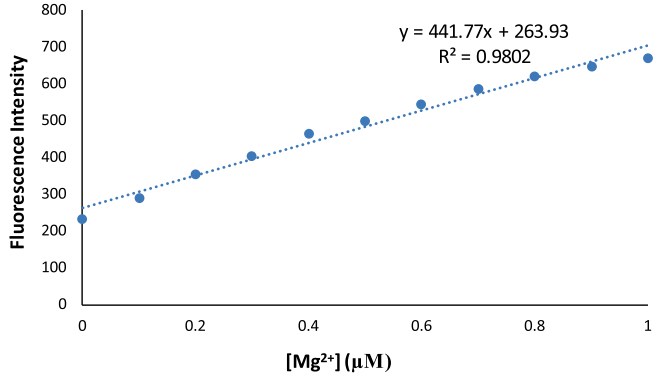

Fig. 10. Linear response curve of H_2L (10 μM) at 490 nm depending on Mg^{2+} concentration.

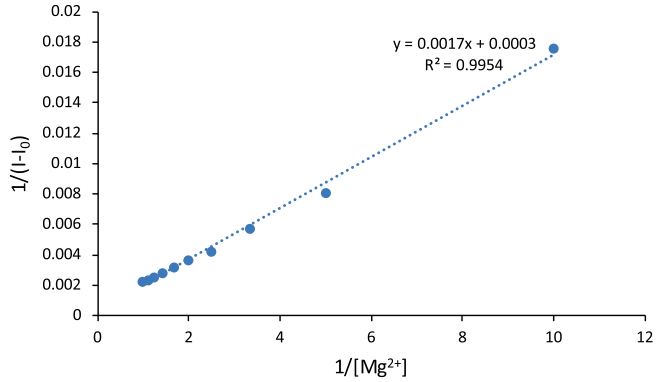

Fig. 11. Benesi-Hildebrand plot of H_2L (10 μM) with Mg^{2+} in EtOH/H_2O (9:1, v/v) solution.

The resulting Benesi–Hildebrand plot, shown in Fig. 8, had a K_a of $1.47 \times 10^6\ M^{-1}$. The K_a obtained illustrates a strong binding ability of Mg^{2+} with the H_2L.

Some of the reported LOD values as well as the related LOD in the present work for Mg^{2+} were collected and compared in Table 1. The results shown in Table 1 indicate on exclusive situation of H_2L among the other chemosensors in terms of lowest LOD value [28–38]. Besides high selectivity, a short response time is necessity for a fluorescent chemosensor. To investigate the response time of the chemosensor to Mg^{2+}, the kinetics of fluorescence enhancement at 490 nm were carried out. The results showed that the response time of H_2L to Mg^{2+} is very fast. When H_2L titrated with Mg^{2+} ions, fast changes in fluorescence intensity were appeared and remained quite stable.

3.7. Absorption spectra and ground state structure

The absorption spectrum of H_2L shows three peaks at ~270 and ~320 nm were attributed to $\pi \rightarrow \pi^*$ transitions associated with the aromatic rings, whereas the broad band from 360 to 460 nm with its maximum centered at 408 nm, which is assigned to the C=N isomerization of the Schiff base.[5]

The UV–Vis absorption spectrum of H_2L in the presence of Mg^{2+} is almost the same as that of sensor H_2L, as shown in Fig. 12. As there is no shift in the band maxima positions, it can be concluded that the change in fluorescence due to the binding of Mg^{2+} to sensor H_2L is a consequence of excited state phenomena.

3.8. Application

H_2L was employed as a fluorescent chemosensor for the determination of Mg^{2+} in drinking water. Results were satisfactory, agreeing with the atomic absorption spectroscopic (AAS) method as shown in Table 2. The percentages of relative error were less than 10%.

3.9. Logic gate operation

H_2L can be applied as a molecular logic gate. The input signals were selected Mg^{2+} (input1) and Fe^{3+} (input 2) and the fluorescence emission at 490 nm as output. When H_2L coordinated with Mg^{2+} (input 1), the fluorescence emission intensity was increased at 490 nm attributing to the typical PET process. The fluorescence intensity was completely quenched upon the continuous addition of Fe^{3+} (input 2). The fluorescence band of H_2L was also quenched when titration was carried out with Fe^{3+} alone. In a positive logic convention, if the fluorescence

Table 1
Comparison of the limit of detection found in the present work with the reported values for Mg^{2+} chemosensors in some of the literatures.

Probe	Medium	LOD (M)	Reference
[2-(quinolin-8′-yloxy) acetyl]hydrazone	Acetonitrile	6.8×10^{-7}	28
2-hydroxy-1-naphthaldehyde derivatives	Aqueous ethanol	2.28×10^{-9}	29
pyridyl-hydrazono-coumarin	Aqueous ethanol	1.05×10^{-7}	30
(E)-N′-((8-hydroxyquinolin-2-yl) methylene) -4-methylbenzohydrazide	DMSO	4.2×10^{-7}	31
(E)-2-(5-allyl-2-hydroxy-3-methoxybenzylidene)-N-phenylhydrazinecarbothioamide	Acetonitrile	8.91×10^{-8}	32
calix[4]arene diamide derivatives	aqueous DMSO	1.3×10^{-5}	33
Schiff base derivatives	DMF	1.0×10^{-7}	34
2-((Z)-1-(2-(2-(1-((Z)-1-(2hydroxynaphthyl)ethylideneamino)propan-2-yl)disulfanyl)ethylimino)ethyl)naphthalen-1-ol	aqueous DMF	5.0×10^{-8}	35
Schiff base derivatives	Ethanol	1.47×10^{-6}	36
β-Hydroxy-α-naphthaldehyde [2-(quinolin-8′-yloxy) acetyl] hydrazone	Acetonitrile	1.0×10^{-7}	37
naphthalene-based	Acetonitrile	1.47×10^{-6}	38
H_2L	Aqueous ethanol	3.0×10^{-9}	Present work

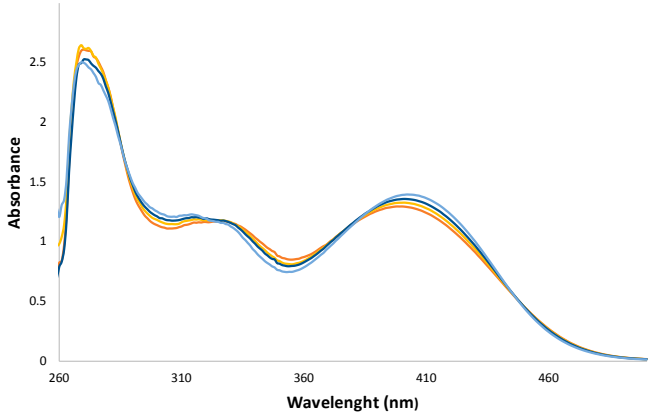

Fig. 12. Changes in the absorption spectra of H_2L (50 μM) as a function of added Mg^{2+} concentration in EtOH/H_2O (9:1, v/v).

Table 2
Determination of Mg^{2+} in drinking water samples.

Drinking waters	AAS method (mg/L)	Proposed method (mg/L)	Relative error (%)
Mineral water	4.4 ± 0.12	4.6 ± 0.12	4.4
Tap water	1.9 ± 0.09	2.1 ± 0.09	10

intensity of 250 was selected as the threshold values, output = 0 when the intensity is lower than 250 and output = 1 when the emission intensity is higher than 250. As discussed above, the intensity of the fluorescence is high enough (output 1 = 1) only under the addition of Mg^{2+} (input 1 = 1 and input 2 = 0). According to the truth table of Fig. 13, the fluorescence responses of H_2L with the two chemical inputs Mg^{2+} and Fe^{3+} satisfy the INHIBIT type logic gate function at the molecular level (Fig. 13).

4. Conclusion

We have developed a new naphthol-based receptor which acts as a fluorescent chemosensor for Mg^{2+} ions. The stoichiometry of [H_2L-Mg^{2+}] complex is 1:1. The association constant of the [H_2L-Mg^{2+}] complex is 1.47×10^6 M^{-1}. The lower detection limit of Mg^{2+} is 3.0×10^{-9} M and indicate on exclusive situation of H_2L among the other chemosensors in terms of lowest LOD value. Molecular logic gates INHIBIT is proposed using Mg^{2+} and Fe^{3+} as inputs.

CRediT authorship contribution statement

Reza Azadbakht: Conceptualization, Project administration, Writing - original draft. **Mostafa Koolivand:** Investigation, Formal analysis. **Saeid Menati:** Validation, Writing - review & editing.

Declaration of Competing Interest

The authors declare that they have no known competing financial interests or personal relationships that could have appeared to influence the work reported in this paper.

Acknowledgments

The authors gratefully acknowledge the Faculty of Chemistry of Bu-Ali Sina University and Ministry of Science Research and Technology.

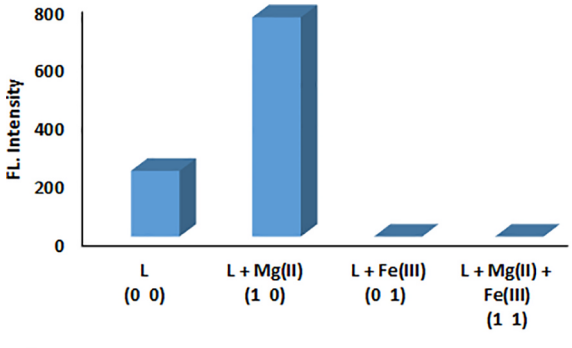

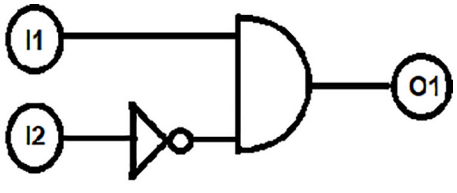

Input 1 Mg^{2+}	Input 2 Fe^{3+}	Output Fluorescence emission at 490 nm
0	0	0
0	1	0
1	0	1
1	1	0

Fig. 13. Logic scheme and the truth table for the proposed INHIBIT type logic gate.

Appendix A. Supplementary data

Supplementary data to this article can be found online at https://doi.org/10.1016/j.ica.2020.120021.

References

[1] R. Swaminathan, Magnesium metabolism and its disorders, Clin. Biochem. Rev. 24 (2003) 47–66.
[2] R.K. Rude, Magnesium, in: A.C. Ross, B. Caballero, R.J. Cousins, K.L. Tucker, T.R. Ziegler (Eds.), Modern Nutrition in Health and Disease, 11th ed., Lippincott Williams & Wilkins, Baltimore, Mass, 2012, pp. 159–175.
[3] S.C. Larsson, M.J. Virtanen, S. Männistö, P. Pietinen, D. Albanes, M.J. Virtamo, Arch. Intern. Med. 168 (2008) 459–465.
[4] N.-E.-L. Saris, E. Mervaala, H. Karppanen, J.A. Khawaja, A. Lewenstam, Magnesium, Clin. Chim. Acta 294 (2000) 1–26.
[5] M. Barbagallo, M. Belvedere, D. Sprini, L.J. Dominguez, Diet and Nutrition in Dementia and Cognitive Decline, Elsevier, 2015.
[6] A.W.C. Yuen, J.W. Sander, EpilepsyRes. 100 (2012) 152–156.
[7] V. Trapani, G. Farruggia, C. Marraccini, S. Iotti, A. Cittadini, F.I. Wolf, Analyst. 135 (2010) 1855–1866.
[8] J. Yin, Y. Hu, J. Yoon, Chem. Soc. Rev. 44 (2015) 4619–4644.
[9] G. Men, C. Chen, S. Zhang, C. Liang, Y. Wang, M. Deng, H. Shang, B. Yang, S. Jiang, Dalton Trans. 44 (2015) 2755–2762.
[10] V.K. Gupta, N. Mergu, L.K. Kumawat, A.K. Singh, Sens. Actuators B Chem. 207 (2015) 216–223.
[11] Z. Liu, H. Xu, S. Chen, L. Sheng, H. Zhang, F. Hao, Spectrochim. Acta. A Mol. Biomol. Spectrosc. 149 (2015) 83–89.
[12] V.K. Gupta, B. Sethi, R.A. Sharma, S. Agarwal, A. Bharti, J. Molecular Liquids 177 (2013) 114–118.
[13] V.K. Gupta, H. Karimi-Maleh, R. Sadegh, Int. J. Electrochem. Sci. 10 (2015) 303–316.
[14] V.K. Gupta, A.K. Singh, L.K. Kumawat, Sens. Actuators B 195 (2014) 98–108.
[15] M.H. Dehghani, D. Sanaei, I. Ali, A. Bhatnagar, J. Molecular Liquids 215 (2016) 671–679.
[16] H. Karimi-Maleh, F. Tahernejad-Javazmi, N. Atar, M. Lütfi Yola, V.K. Gupta, A.A. Ensafi, Ind. Eng. Chem. Res. 54 (2015) 3634–3639.
[17] A. Asfaram, M. Ghaedi, S. Agarwal, I. Tyagi, V.K. Gupta, RSC Adv. 5 (2015) 18438–18450.
[18] (a) Y. Suzuki, H. Komatsu, T. Ikeda, N. Saito, S. Araki, D. Citterio, H. Hisamoto, Y. Kitamura, T. Kubota, J. Nakagawa, K. Oka, K. Suzuki, Anal. Chem. 74 (2002) 1423–1428;
(b) H. Komatsu, T. Miki, D. Citterio, T. Kubota, Y. Shindo, Y. Kitamura, K. Oka, K. Suzuki, J. Am. Chem. Soc. 127 (2005) 10798–10799;
(c) H.M. Kim, P.R. Yang, M.S. Seo, J.S. Yi, J.H. Hong, S.-J. Jeon, Y.-G. Ko, K.J. Lee, B.R. Cho, J. Org. Chem. 72 (2007) 2088–2096;
(d) E. Brunet, M.T. Alonso, O. Juannes, R. Sedano, J.C. Rodriguez-Ubis, Tetrahedron Lett. 38 (1997) 4459–4462;
(e) L.F. Capitan-Vallvey, M.D. Fernandez-Ramos, A. Lapresta-Fernandez, E. Brunet, J.C. Rodriguez-Ubis, O. Juanes, Talanta 68 (2006) 1663–1670.
[19] (a) D. Ray, P.K. Bharadxwaj, Inorg. Chem. 47 (2008) 2252–2254;
(b) Z.D. Liu, H.J. Xu, C.F. Song, D.Q. Huang, L.Q. Sheng, R.H. Shi, Chem. Lett. 40 (2011) 75–77;
(c) L.N. Wang, W.W. Qin, X.L. Tang, W. Dou, W.S. Liu, J. Phys. Chem. A 115 (2011) 1609–1616.
[20] (a) T. Shoda, K. Kikuchi, H. Kojima, Y. Urano, H. Komatsu, K. Suzuki, T. Nagano, Analyst 128 (2003) 719–723;
(b) H. Komatsu, N. Iwasawa, D. Citterio, Y. Suzuki, T. Kubota, K. Tokuno, Y. Kitamura, K. Oka, K. Suzuki, J. Am. Chem. Soc. 126 (2004) 16353–16360;
(c) G. Farruggia, S. Iotti, L. Prodi, M. Montalti, N. Zaccheroni, P.B. Savage, V. Trapani, P. Sale, F.I. Wolf, J. Am. Chem. Soc. 128 (2006) 344–350;
(d) H. Hama, T. Morozumi, H. Nakamura, Tetrahedron Lett. 48 (2007) 1859–1861;
(e) X.H. Dong, J.H. Han, C.H. Heo, H.M. Kim, Z.H. Liu, B.R. Cho, Anal. Chem. 84 (2012) 8110–8113;
(f) S.C. Schwartz, B. Pinto-Pacheco, J.P. Pitteloud, D. Buccella, Inorg. Chem. 53 (2014) 3204–3209.
[21] (a) X.M. He, E.C.C. Cheng, N.Y. Zhu, V.W.W. Yam, Chem. Commun. 27 (2009) 4016–4018;
(b) X. Zhu, C. He, D.P. Dong, Y. Liu, C.Y. Duan, Dalton Trans. 39 (2010) 10051–10055;
(c) Y. Dong, J.F. Li, X.X. Jiang, F.Y. Song, Y.X. Cheng, C.J. Zhu, Org. Lett. 13 (2011) 2252–2255;
(d) M. Tian, H. Ihmels, S. Ye, Org. Biomol. Chem. 10 (2012) 3010–3018;
(e) C. Marraccini, G. Farruggia, M. Lombardo, L. Prodi, M. Sgarzi, V. Trapani, C. Trombini, F.I. Wolf, N. Zaccheroni, S. Iotti, Chem. Sci. 3 (2012) 727–734;
(f) L. Zhao, Y. Liu, C. He, J. Wang, C. Duan, Dalton Trans. 43 (2014) 335–343;
(g) A. Sargenti, G. Farruggia, E. Malucelli, C. Cappadone, L. Merolle, C. Marraccini, G. Andreani, L. Prodi, N. Zaccheroni, M. Sgarzi, C. Trombini, M. Lombardo, S. Iotti, Analyst 139 (2014) 1201–1207.
[22] (a) K.C. Song, M.G. Choi, D.H. Ryu, K.N. Kim, S.K. Chang, Tetrahedron Lett. 48 (2007) 5397–5400;
(b) N. Singh, N. Kaur, R.C. Mulrooney, J.F. Callan, Tetrahedron Lett. 49 (2008) 6690–6692.
[23] K. Rout, A.K. Manna, M. Sahu, G.K. Patra, Inorg. Chim. Acta 486 (2019) 733–741.
[24] M.S. Kim, T. GeunJo, M. Yang, J. Han, M.H. Lim, C. Kim, Spectrochim. Acta. A Mol. Biomol. Spectrosc. 211 (2019) 34–43.
[25] V. Raju, R. Selva Kumar, Y. Tharakeswar, S.K. Ashok Kumar, Inorg. Chim. Acta 493 (2019) 49–56.
[26] R. Azadbakht, M. Koolivand, J. Khanabadi, Anal. Methods 9 (2017) 4688–4694.
[27] L.K. Kumawat, N. Mergu, M. Asif, V.K. Gupta, Sens. Actuators B Chem. 231 (2016) 847–859.
[28] J.-C. Qin, Z.-Y. Yang, L. Fan, B.-D. Wang, Spectrochim. Acta. A Mol. Biomol. Spectrosc. 140 (2015) 21–26.
[29] Z. Liu, H. Xu, S. Chen, L. Sheng, H. Zhang, F. Hao, P. Su, W. Wang, Spectrochim. Acta. A Mol. Biomol. Spectrosc. 149 (2015) 83–89.
[30] J. Orrego-Hernández, N. Nuñez-Dallos, J. Portilla, Talanta 152 (2016) 432–437.
[31] P. Marimuthu, A. Ramu, Sens. Actuators B Chem. 266 (2018) 384–391.
[32] M. Patil, K. Keshav, M.K. Kumawat, S. Bothra, S.K. Sahoo, R. Srivastava, J. Rajput, R. Bendre, A. Kuwar, J. Photoch. Photobio. A 364 (2018) 758–763.
[33] K.C. Song, M.G. Choi, D.H. Ryu, K.N. Kim, S.-K. Chang, Tetrahedron Lett. 48 (2007) 5397–5400.
[34] P.S. Hariharan, S.P. Anthony, RSC Adv. 4 (2014) 41565–41571.
[35] G. Tamil Selvan, V. Chitra, Israel V.M.V. Enocha, P. Mosae Selvakumar, New J. Chem. 42 (2018) 902–909.
[36] T. Yu, P. Sun, Y. Hu, Y. Ji, H. Zhou, B. Zhang, Y. Tian, J. Wu, Biosensors Bioelectronics 86 (2016) 677–682.
[37] J.-C. Qin, Z.-Y. Yang, L. Fan, B.-D. Wang, Spectrochim. Acta A Mol. Biomol. Spectrosc. 140 (2015) 21–26.
[38] J.-C. Qin, Z.-Y. Yang, G.-Q. Wang, Inorg. Chim. Acta 435 (2015) 194–199.